Imposing control on self-assembly: rational design and synthesis of a mixed-metal, mixed-ligand coordination cage containing four types of component

Alexander J. Metherell and Michael D. Ward

Supporting Information

1. Experimental information

General details

Metal salts and all organic reagents were purchased from Alfa or Sigma-Aldrich and used as received. ^{1}H NMR spectra were recorded on Bruker DRX 500 MHz, Bruker AV-III 400 MHz or AV-1 800 MHz instruments. Low-resolution electrospray mass spectra were recorded on a Micromass LCT instrument. High-resolution electrospray mass spectra were measured on an electron transfer dissociation (ETD) enabled ThermoFisher-Scientific Orbitrap Elite, equipped with an HESI source (ThermoFisher Scientific). UV/Vis absorption spectra were measured on a Cary 50 spectrophotometer.

Preparation of $[Ru_4Cd_{12}(L^{ph})_{12}(L^{naph})_{12}](PF_6)_7(BF_4)_{25}$

To a stirred solution of *fac*-$[Ru(L^{ph})_3](PF_6)_2$ (0.023 g, 0.015 mmol; preparation in ref 1) in nitromethane (10 cm^3) was added $[Cd_3(L^{naph})_3](BF_4)_6$ (0.035 g, 0.015 mmol; preparation in ref. 6, main text). The initially turbid solution became clear after heating at 60 ^{o}C for 1 hour, after which the mixture was passed through a membrane filter. Slow diffusion of di-isopropyl ether into the nitromethane solution yielded the complex as large yellow blocks of X-ray quality, which were separated from the mother liquor and washed with di-isopropyl ether. Yield: 0.022 g, 40 %. ESMS (selected peaks): *m/z* 2835, $([Ru_4Cd_{12}(L^{ph})_{12}(L^{naph})_{12}](BF_4)_{26}(PF_6))^{5+}$; 2348, $([Ru_4Cd_{12}(L^{ph})_{12}(L^{naph})_{12}](BF_4)_{25}(PF_6))^{6+}$; 2000, $([Ru_4Cd_{12}(L^{ph})_{12}(L^{naph})_{12}](BF_4)_{24}(PF_6))^{7+}$. UV/Vis in MeCN [$\lambda_{max}$/nm ($10^{-3}$ ε/M^{-1} cm^{-1})]: 397 (50.3), 287 (577.0), 229 (783.8). Note that the extinction coefficient associated with the Ru-based MLCT absorption at 397 nm is *ca.* four times more intense than for mononuclear *fac*-$[Ru(L^{ph})_3](PF_6)_2$ (ref. 12, main text).

2. Bond distances (Å) around the metal ions from the crystal structure

Cd(1)-N(11K)	2.298(9)	Cd(2)-N(11D)	2.275(8)
Cd(1)-N(11E)	2.313(8)	Cd(2)-N(31C)	2.310(8)
Cd(1)-N(22E)	2.327(8)	Cd(2)-N(42C)	2.316(10)
Cd(1)-N(22K)	2.342(10)	Cd(2)-N(42V)	2.329(10)
Cd(1)-N(22B)	2.345(8)	Cd(2)-N(22D)	2.380(8)
Cd(1)-N(11B)	2.358(8)	Cd(2)-N(31V)	2.418(11)
Cd(4)-N(11Q)	2.287(9)	Cd(6)-N(42E)	2.278(10)
Cd(4)-N(41N)	2.298(9)	Cd(6)-N(31F)	2.283(9)
Cd(4)-N(31D)	2.317(11)	Cd(6)-N(31E)	2.295(11)
Cd(4)-N(22Q)	2.347(9)	Cd(6)-N(42F)	2.338(9)
Cd(4)-N(42D)	2.360(11)	Cd(6)-N(11H)	2.357(11)
Cd(4)-N(31N)	2.377(10)	Cd(6)-N(22H)	2.381(12)
Cd(9)-N(11L)	2.248(10)	Cd(10)-N(42W)	2.231(11)
Cd(9)-N(11M)	2.291(11)	Cd(10)-N(31M)	2.298(10)
Cd(9)-N(22L)	2.302(9)	Cd(10)-N(22T)	2.315(11)
Cd(9)-N(42A)	2.309(10)	Cd(10)-N(11T)	2.321(9)
Cd(9)-N(22M)	2.356(10)	Cd(10)-N(31W)	2.351(13)
Cd(9)-N(31A)	2.374(11)	Cd(10)-N(42M)	2.373(11)
Cd(11)-N(42G)	2.258(13)	Cd(12)-N(42P)	2.246(10)
Cd(11)-N(11R)	2.284(10)	Cd(12)-N(42R)	2.269(13)
Cd(11)-N(42O)	2.315(12)	Cd(12)-N(31R)	2.306(12)
Cd(11)-N(31O)	2.329(10)	Cd(12)-N(31P)	2.316(12)
Cd(11)-N(22R)	2.340(9)	Cd(12)-N(31X)	2.341(13)
Cd(11)-N(31G)	2.412(12)	Cd(12)-N(42X)	2.374(12)
Cd(14)-N(31J)	2.257(13)	Cd(15)-N(42I)	2.221(16)
Cd(14)-N(22C)	2.287(10)	Cd(15)-N(42T)	2.283(13)
Cd(14)-N(31Q)	2.297(11)	Cd(15)-N(31L)	2.283(9)
Cd(14)-N(42Q)	2.303(13)	Cd(15)-N(42L)	2.329(9)
Cd(14)-N(11C)	2.321(10)	Cd(15)-N(31T)	2.364(10)
Cd(14)-N(42J)	2.399(12)	Cd(15)-N(31I)	2.388(12)
Cd(16)-N(11F)	2.245(14)	Cd(7)-N(11O)	2.293(9)
Cd(16)-N(22F)	2.297(14)	Cd(7)-N(11P)	2.319(10)
Cd(16)-N(31K)	2.312(12)	Cd(7)-N(22P)	2.322(10)
Cd(16)-N(42K)	2.330(11)	Cd(7)-N(42U)	2.339(10)
Cd(16)-N(42S)	2.337(16)	Cd(7)-N(22O)	2.359(9)
Cd(16)-N(31S)	2.41(2)	Cd(7)-N(31U)	2.360(12)
Ru(3)-N(11V)	2.022(9)	Ru(5)-N(22J)	2.036(9)
Ru(3)-N(22V)	2.032(8)	Ru(5)-N(11G)	2.043(9)
Ru(3)-N(22A)	2.038(9)	Ru(5)-N(31H)	2.046(11)
Ru(3)-N(42B)	2.075(8)	Ru(5)-N(22G)	2.058(10)
Ru(3)-N(31B)	2.083(9)	Ru(5)-N(11J)	2.074(9)
Ru(3)-N(11A)	2.089(9)	Ru(5)-N(42H)	2.083(9)
Ru(8)-N(22S)	2.029(10)	Ru(13)-N(11I)	1.988(13)
Ru(8)-N(22U)	2.059(9)	Ru(13)-N(22N)	2.053(10)
Ru(8)-N(11W)	2.072(10)	Ru(13)-N(11N)	2.071(12)
Ru(8)-N(22W)	2.083(9)	Ru(13)-N(22X)	2.074(9)
Ru(8)-N(11U)	2.100(10)	Ru(13)-N(11X)	2.098(11)
Ru(8)-N(11S)	2.108(8)	Ru(13)-N(22I)	2.109(11)

3. High-resolution electrospray mass spectra of selected signals

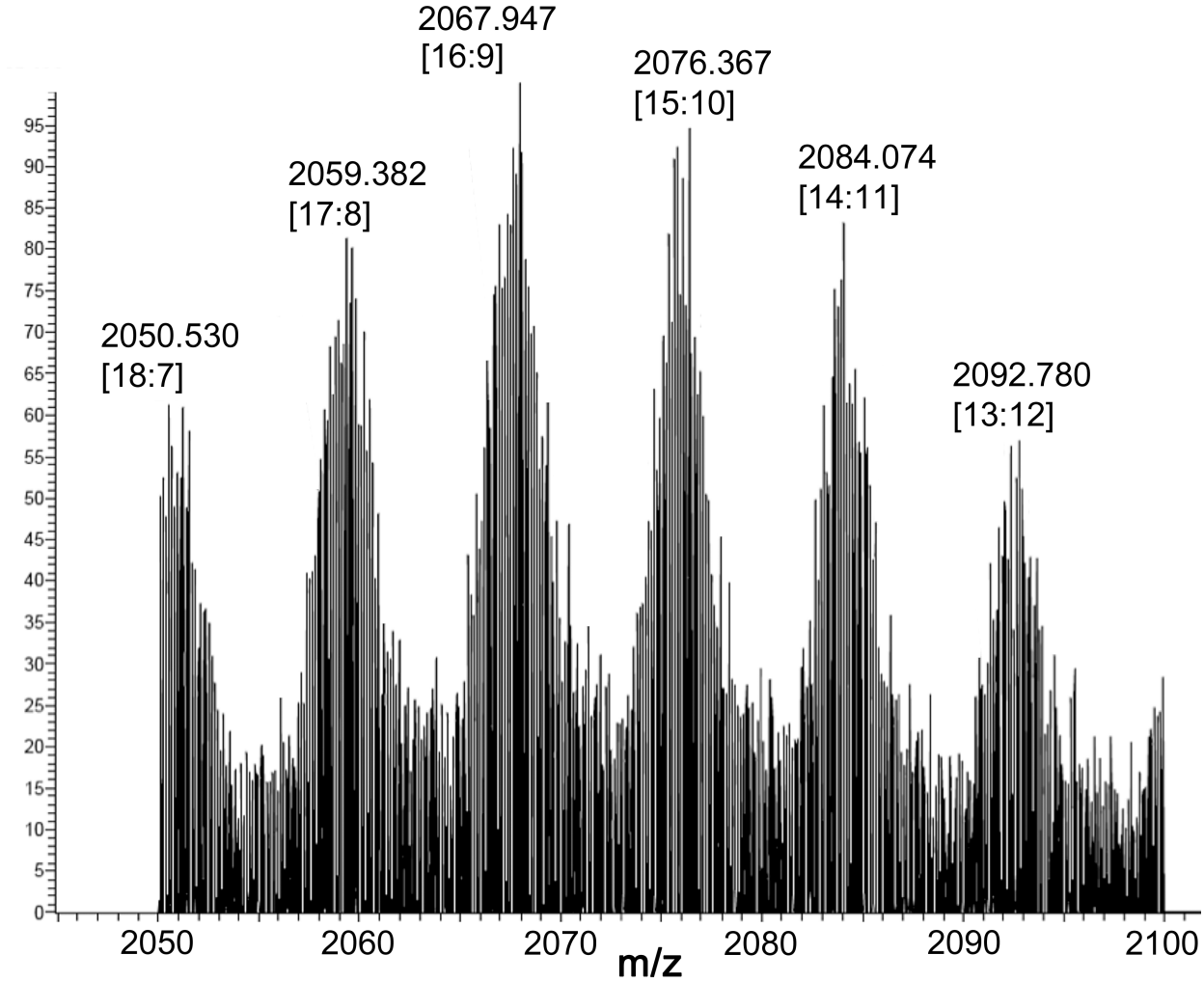

Figure S1 High resolution ES mass spectrum of the cage in the region showing 7+ ions, showing the series of signals for $\{[Ru_4Cd_{12}(L^{ph})_{12}(L^{naph})_{12}](BF_4)_x(PF_6)_y\}^{7+}$ where $x + y = 25$. For each cluster the values in square brackets [x:y] are the numbers of each type of anion.

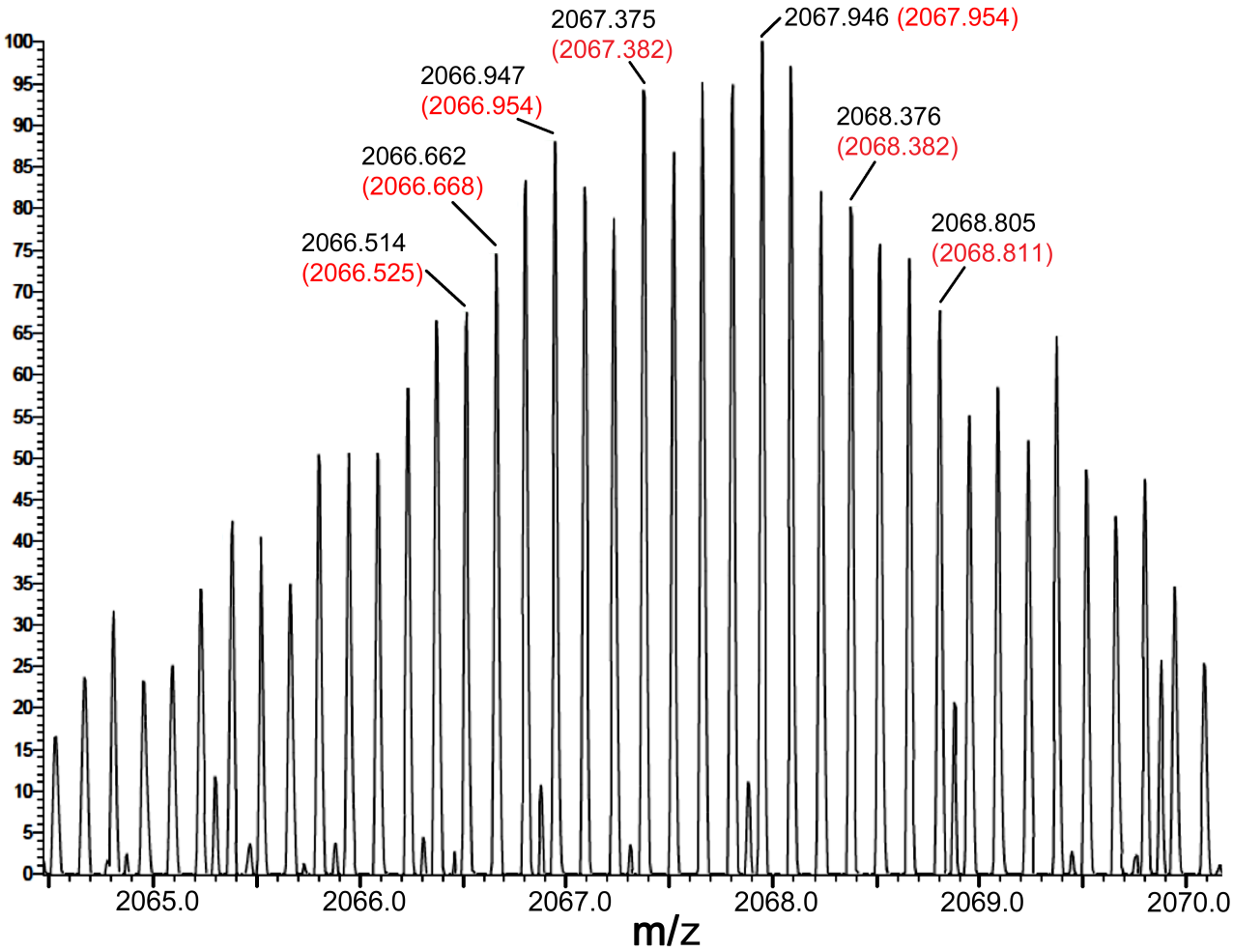

Figure S2 Expansion of the region in Fig. S1 corresponding to the species $\{[Ru_4Cd_{12}(L^{ph})_{12}(L^{naph})_{12}](BF_4)_{16}(PF_6)_9\}^{7+}$, showing the 1/7 mass unit isotopic spacing and the good agreement with calculated *m/z* values (shown in red).

4. Additional NMR data

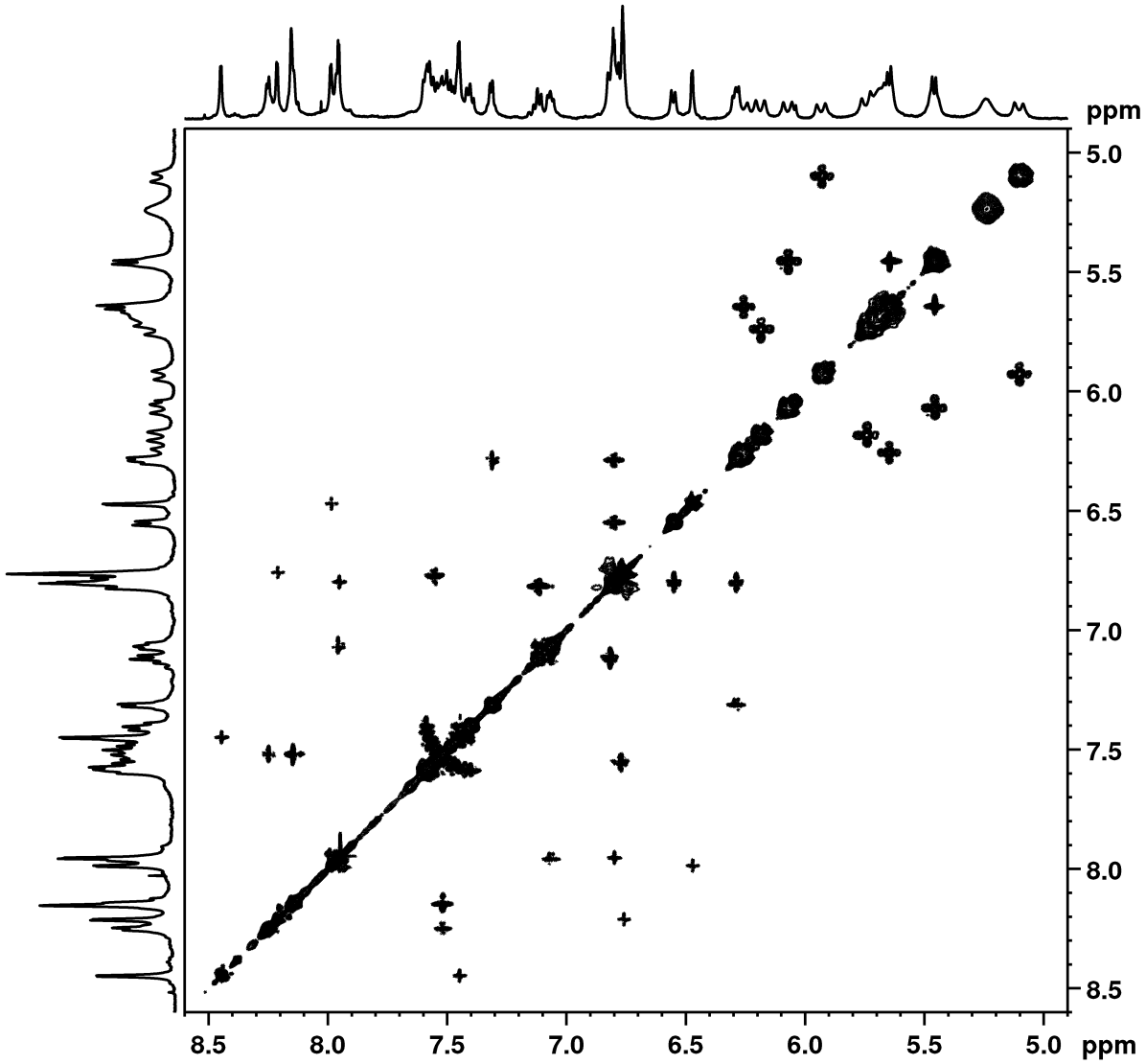

Figure S3 COSY spectrum (500 MHz, 298K) of $[Ru_4Cd_{12}(L^{ph})_{12}(L^{naph})_{12}](PF_6)_7(BF_4)_{25}$ in CD_3NO_2.

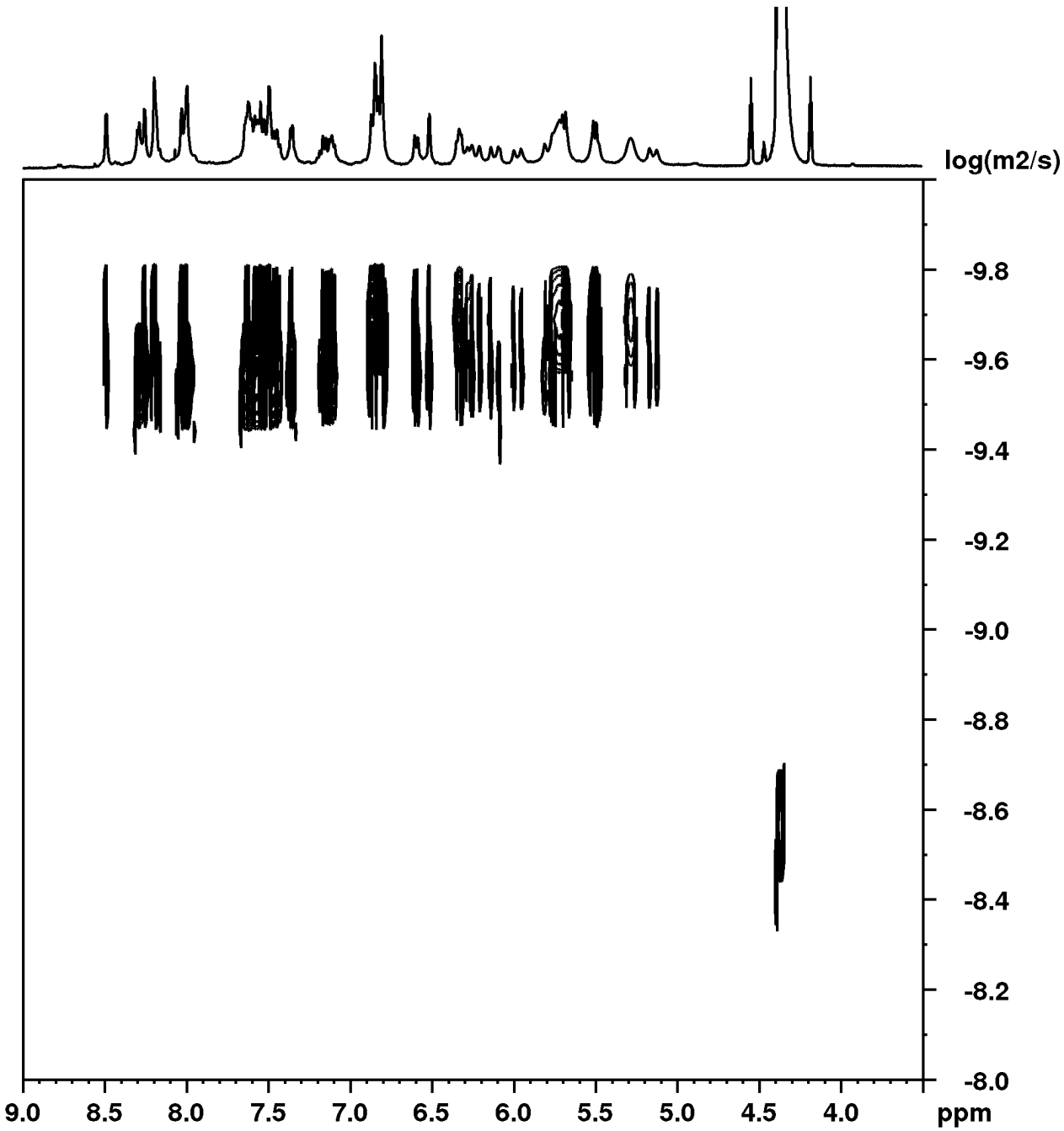

Figure S4 DOSY spectrum (400 MHz, 298K) of $[Ru_4Cd_{12}(L^{ph})_{12}(L^{naph})_{12}](PF_6)_7(BF_4)_{25}$ in CD_3NO_2.

5. Additional figures of the crystal structure of $[Ru_4Cd_{12}(L^{ph})_{12}(L^{naph})_{12}](PF_6)_7(BF_4)_{25}$

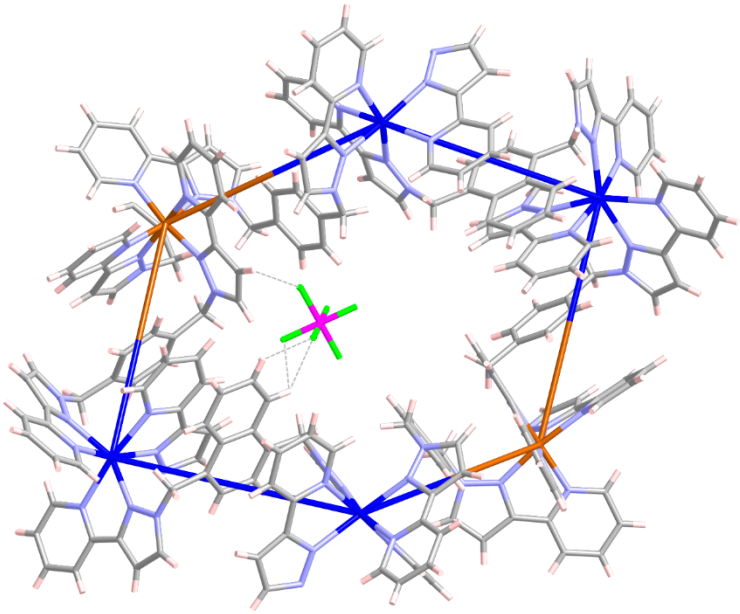

Figure S5 View of one of the large Ru_2Cd_4 windows of $[Ru_4Cd_{12}(L^{ph})_{12}(L^{naph})_{12}](PF_6)_7(BF_4)_{25}$, with an associated $[PF_6]^-$ anion forming C-H…F contacts with the surface of the cage.

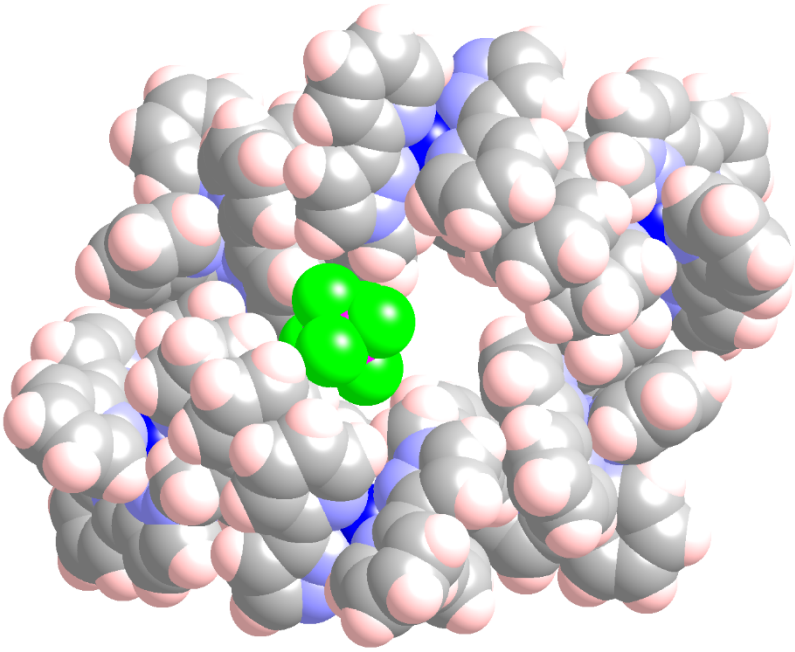

Figure S6 Space-filling version of Fig. S5

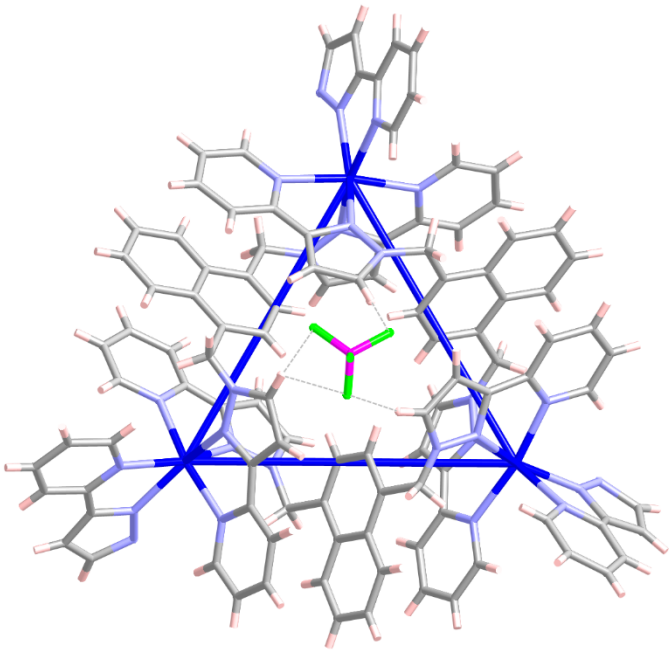

Figure S7 View of one of the Cd_3 windows, with an associated $[BF_4]^-$ anion forming C-H…F contacts with the surface of the cage.

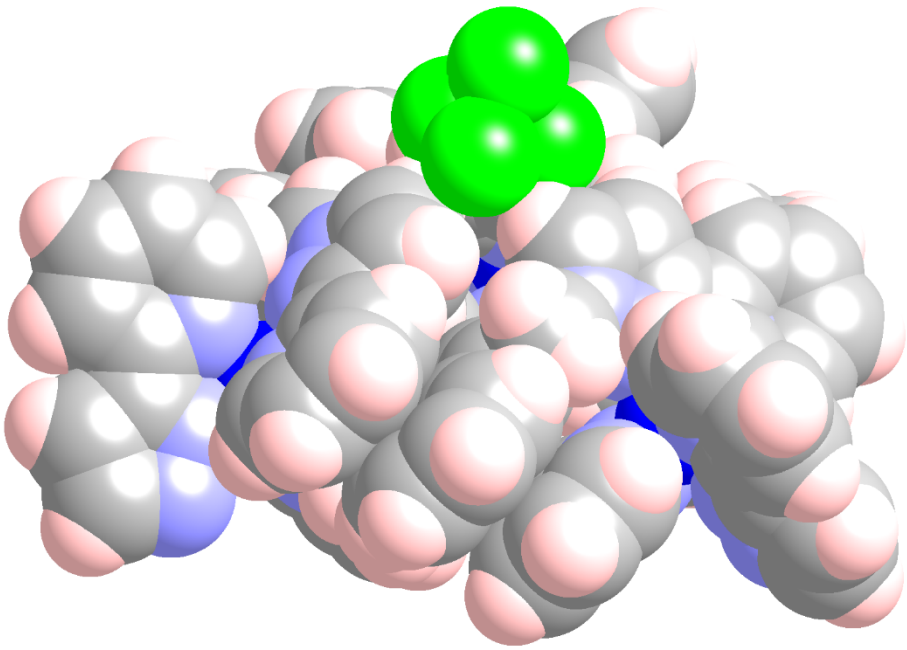

Figure S8 Spacefilling view of Fig. S7 from a different orientation.